IN VITRO FUSION OF *ACANTHAMOEBA* PHAGOLYSOSOMES

II. Quantitative Characterization of In Vitro Vacuole Fusion by Improved Electron Microscope and New Light Microscope Techniques

PETER J. OATES and OSCAR TOUSTER

From the Department of Molecular Biology, Vanderbilt University, Nashville, Tennessee 37235

ABSTRACT

To investigate the properties of phagolysosome (PL) fusion in *Acanthamoeba* homogenates, it was necessary to develop reliable methods for measuring in vitro PL fusion. The need to distinguish PL fusion from PL adhesion was met by the development of a quantitative electron microscope assay. Initial characterization of the fusion reaction by this method was followed by the development of a more rapid light microscope assay. Results obtained by the two methods were found to be in close agreement.

By use of these new techniques, the in vitro PL fusion reaction was demonstrated to occur in a quantitatively reproducible manner. Under the present conditions employed, PL breakdown was not detected at any time during the in vitro incubation, while PL fusion was observed to proceed linearly for ~10 min, at which time the reaction ceased. Incubation of mixtures of two distinct PL types resulted in increases in hybrid PL types that were paralleled by decreases in nonhybrid PL types. The relative changes in PL concentrations observed were quantitatively consistent with PL fusion occurring randomly with respect to PL type. PL fusion was strongly inhibited by low concentrations of KF (50% inhibition at 2.7 mM), and by approximately tenfold higher concentrations of KCl, while KCN and 2,4-dinitrophenol (2,4-DNP) had little effect. In addition to further defining the nature of the PL fusion reaction in this system, these results demonstrate that, by use of the techniques described, quantitative study of the biochemical properties of this reaction is now possible.

KEY WORDS membrane fusion · lysosome function · lysosome fusion · EM methodology · *Acanthamoeba*

It is well documented that fusion processes involving the membranes of subcellular organelles play a fundamental role in a wide variety of physiological and pathological mechanisms (3, 4, 7, 12). However, largely due to the lack of a suitable experimental system, the biochemical and biophysical factors which govern organelle membrane fusion are poorly understood (12).

We have previously presented evidence that fusion of subcellular vacuoles, phagolysosomes (PLs),[1] will occur during the incubation of PL-rich

[1] *Abbreviations used in this paper:* BPB, Bromphenol blue; DDF, dye-diluting fluid; DF, diluting fluid; 2,4-DNP, 2,4-dinitrophenol; EM, electron microscopy; GGRBC, glutaraldehyde-fixed goat erythrocyte; Hv,

homogenates of the small soil amoeba, *Acanthamoeba* sp. (Neff) (11). This in vitro vacuole fusion reaction was observed to occur relatively rapidly, in a time- and temperature-dependent manner, in significant yield, in the absence of exogenous fusion-inducing agents, and, in its initial stages, in the absence of apparent membrane damage (11). In addition, the reaction appeared to be independent of the type of material within the vacuoles, to retain the specificity of fusion between membrane types that was observed in vivo, and to occur by a mechanism morphologically similar or identical to that observed in vivo (11). Since these properties closely resemble the known and presumed properties of vacuole fusion in vivo (3, 4), this in vitro system appeared to be a promising experimental model of the process of intracellular organelle membrane fusion. It was therefore of interest to further develop and characterize this system. A step that was clearly necessary was the development of reliable methods for measuring the extent of PL fusion under various experimental conditions.

We report here the accomplishment of these objectives. Drawing on the concepts discussed by Sjöstrand (15), Baudhuin et al. (1), and others (2, 9, 18), we have developed new techniques for the measurement of PL fusion by transmission electron microscopy (EM). We also report here the development of a considerably faster assay for PL fusion, performed by light microscopy (LM) and validated by the EM assay. Results obtained by these methods concerning some of the basic characteristics and biochemical properties of the PL fusion reaction in *Acanthamoeba* homogenates are also presented.

MATERIALS AND METHODS

Materials

B.E.E.M. capsules (size 00), propylene oxide, and parallel-bar grids (no. R-200 or R-300) were purchased from Ernest F. Fullam, Inc., Schenectady, N. Y. Nuclepore filters were obtained from the Nuclepore Corp., Pleasanton, Calif. EM grade OsO_4, biological grade glutaraldehyde, and Epon embedding materials were obtained from Polysciences, Inc., Warrington, Pa. The composition of the Epon mixture used was a slight modification of that employed by Wetzel and Korn (17): Epon 812, 51.6% (wt/wt); nadic methyl anhydride, 36.6% (wt/wt); dodecenylsuccinic anhydride, 11.8% (wt/wt); and 0.15–0.17% (vol/vol) 2,4,6-tri(dimethylaminomethyl)-phenol (DMP-30). Enzyme grade Tris (base) was obtained from Becton, Dickinson & Co., Schwarz/Mann Div., Orangeburg, N. Y. Bromphenol blue (BPB) and Certified Eosin Y was purchased from American Hospital Supply Corp., Harleco Div., Gibbstown, N. J. Other chemicals were reagent grade.

Cell Cultures and Marker Particles

Acanthamoeba sp. (Neff) were grown axenically at 30°C in 500-ml and 1-liter aerated cultures as described previously (11). *Saccharomyces cerevisiae* (Anheuser-Busch strain) were grown and prepared for ingestion by *Acanthamoeba* as described before (11). Small portions (2–3 ml) of autoclaved yeast at 4–6 × 10^9 yeast/ml were frozen in a dry ice-acetone mixture and stored at −85°C until use. Glutaraldehyde-fixed goat erythrocytes (GGRBC) were prepared with the following modifications of the previously described procedure (11). The suspending medium used throughout was 0.75% NaCl which was 10 mM in potassium phosphate buffer, pH 6.8 (PBS2). After the initial washes, each pellet was resuspended with 11 ml of PBS2. The suspensions were then pooled in a flask on a magnetic stirrer, and 200 ml of 2.2% glutaraldehyde was slowly added to the stirring suspension, which was then stirred continuously at room temperature for ~24 h. The fixed erythrocytes were then washed with PBS2 in the manner previously reported. The final pellets were resuspended to 2–5 × 10^9 cells/ml (7–9 ml/tube), frozen in a dry ice-acetone mixture, and stored at −85°C. Immediately before use, the thawed suspensions were centrifuged for 10 min at 2,100 rpm (975 *g*) in a model PR-2 International centrifuge (International Equipment Co., Needham Heights, Mass.). The resulting pellets were resuspended 1:3 (vol/vol) with PBS2, giving a GGRBC particle concentration of ~1 × 10^{10}/ml. (In this report, all dilutions and resuspensions [e.g., 1:3] were made on a direct [vol/vol] basis.)

In Vitro Fusion Experiments

In vitro phagolysosome fusion experiments were performed essentially as described previously (11), with the following modifications in procedure. From a 500-ml culture of *Acanthamoeba* at 3–6 × 10^5 cells/ml, 2 × 10^8 cells were harvested and divided equally into two bubbler tubes at a concentration of 1 × 10^7 cells/ml. After ingestion of GGRBC particles by the cells in one culture and yeast particles by the cells in the other, the two cultures were separately washed as described (11). The final cell pellets (0.8–1.0 ml each) were resuspended 1:1 with ice-cold 0.05 M Tris-HCl, pH 8.0 (at 23°C), and each of the two suspensions was immediately transferred to a separate 2-ml Dounce homogenizer (Kontes Co.,

hybrid vacuole; LM, light microscopy; PBS2, phosphate buffered saline; PBSM, phosphate buffered saline with 1 mM $CaCl_2$ and $MgSO_4$; PL, phagolysosome (vacuole); Rv, GGRBC-containing vacuole; Yv, vacuole containing autoclaved yeast cell(s).

Vineland, N. J.) on ice. 5–8 min later, each homogenizer was placed in a prechilled rubber adapter (no. 302, DuPont Instruments-Sorvall, DuPont Co., Wilmington, Del.), and was centrifuged for 5 min at 2,100 rpm (975 *g*) in a model PR-2 International centrifuge (0–4°C). The supernates were removed, and the swollen, packed cells were each separately homogenized with 1–3 strokes of a tight Dounce pestle (>95% cell breakage). In most experiments, 0.3–0.4-ml aliquots of each of the phagolysosome-rich homogenates were combined into one test tube on ice. Aliquots (usually 25 μl) from this mixture were then pipetted into individual 12 × 75 mm test tubes also on ice. Solutions of compounds to be added to the homogenate mixtures were adjusted to ~pH 7.0, and 1–2-μl aliquots of the neutralized solutions were added to the homogenate mixtures 15–30 min before incubation. Tubes containing KCN were tightly capped. Reactions were initiated by vortexing 3–5 s and placing the tubes in a shaking incubator at 30–32°C. Reactions were terminated by a 1:6 dilution with ice-cold 0.84% NaCl which was 10 mM in potassium phosphate buffer and 1 mM in $CaCl_2$ and $MgSO_4$, pH 6.8 (PBSM) or, in most cases, with ice-cold filtered *Acanthamoeba* cytoplasm containing 4 mM KF, pH 6.6–7.1 (see below). The tubes were vortexed 3–5 s and placed on ice. Mixtures were then analyzed by LM and EM as described below.

Preparation of Cytoplasm

A 1-liter culture of *Acanthamoeba* at 8–20 × 10^5 cells/ml was harvested, and the cell pellets were resuspended in 0.05 M Tris-HCl, pH 8.0 in a final combined volume of 40 ml. The pooled cells were then centrifuged in a model PR-2 International centrifuge at 1,000 *g* for 5 min. The supernate was removed and the loose cell pellet (1.0–1.4 × 10^8 cells/ml pellet) was transferred into a 50-ml Dounce homogenizer on ice. The swollen, packed cells were disrupted with 7 or 8 up-and-down strokes with a tight pestle, and the homogenate was filtered through a 3 μm pore Nuclepore filter mounted in a precooled 47 mm Swin-Lok holder (Nuclepore Corp.). KF was added to the filtrate to a final concentration of 4 mM. This preparation, "diluting fluid" (DF), was then used as a reagent for diluting the homogenates and handling the vacuoles. Besides maintaining a constant pH in the DF by inhibiting glycolysis, the fluoride was also intended to prevent further PL fusion in samples thus diluted (see Results). The pH of DF was 6.7 ± 0.2 (mean ± SD, 10 preparations). This reagent was always freshly prepared on the same day that a fusion experiment was run. Eosin Y was prepared as a 6% (wt/vol) stock solution in PBSM and filtered through a 0.45-μm-pore Millex unit (Millipore Corp., Medford, Mass.) before use.[2] Dye-diluting fluid mixture (DDF) was prepared by combining the filtered dye solution with DF in appropriate proportions. The standard DDF preparation has a final dye concentration of 0.34%.

Electron Microscopy

To circumvent the problem of nonrepresentative sampling that is inherent in conventional EM preparative methods (1, 15), vacuole samples taken from homogenate mixtures were prepared for EM as relatively thin, uniform pellicles (1, 15, 18). The pellicles were protected from erosion during dehydration and embedding by an overlying Nuclepore filter (cf. 18). Specimen particles were deposited as pellicles either by filtration (using specially designed filtration capsules), or, most recently, by sedimentation (using specially designed sedimentation capsules). Both methods of pellicle preparation have given similar results. The details of the filtration method, which was developed specifically for application to particles that are several μm in diameter (i.e., yeast- and GGRBC-containing vacuoles), are given below. The details of the sedimentation method, which was developed for application to subcellular fractions in general, will be fully described in a forthcoming report.[3] Unless otherwise stated, a dimension given in the paragraphs below refers to the (outer) diameter of an object.

CONSTRUCTION OF FILTRATION CAPSULES: Filtration capsules were constructed from standard B.E.E.M capsules. The pointed end of a B.E.E.M capsule was cut off, the cap was detached, and a 5-mm hole was cut in the center of the cap (no. 2 cork borer). The lower portion of the capsule wall was slightly expanded by being fitted over the end of an 8.0-mm aluminum rod, immersed in boiling water for 1 min, cooled, and removed from the rod (see Fig. 1). The detached, bored cap, filter support piece (FSP), was heat-treated in a similar fashion. The bottom of the tapered capsule wall then fitted flush with the FSP, with negligible mechanical stress between the two. Using a no. 4 cork borer, 9-mm discs were punched out of Nuclepore filters (0.8 μm pore size). A small amount of epoxy glue (3M Co., St. Paul, Minn.) was then applied to the inner surface of the FSP. A filter disc was then placed on the FSP, the capsule wall was inserted, and the epoxy was allowed to harden (Fig. 1). Processing plugs (see Fig. 1) were constructed from polyethylene tubing (7.9 mm o.d. with 1.6 mm thick walls) which was cut to give pieces 14 mm long with flat, square-cut ends. A straight, V-shaped lateral groove (~0.7 mm deep, 1 mm wide at the plug surface) was cut along opposite sides of each piece (Fig. 1). A 7-mm Nuclepore filter (no. 3 punch) was then glued to one end of the plug, care being taken to

[2] Dye concentrations given have not been corrected for impurities (11%) in the certified dye or for the slight loss because of absorption of the dye to the matrix of the Millex filter.

[3] P. J. Oates, manuscript in preparation. The key features of the sedimentation technique have recently been described in abstract form (10).

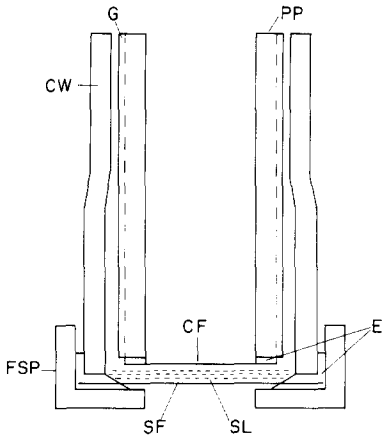

FIGURE 1 Schematic diagram of a filtration capsule with the processing plug (*PP*) inserted. The spacings between the parts are exaggerated for the sake of clarity. See text for details. *CW*, capsule wall; *FSP*, filter support piece; *SF*, specimen filter; *SL*, specimen layer; *CF*, covering filter; *E*, hardened epoxy; *G*, lateral groove.

apply only the minimum amount of epoxy necessary to make a complete seal.

SAMPLE FILTRATION AND PROCESSING PLUG INSERTION: Filtration capsules (without the processing plugs) were inserted from below into snugly-fitting vertical holes located in the upper horizontal section of a leveled plexiglass rack, which had been built for this purpose. The open-sided, rectangular rack was 35 cm long × 6.5 cm wide × 10 cm high, with 20 9-mm holes drilled vertically through the 6 mm thick upper horizontal section. Samples (50–200 μl) containing 1–6 × 10^7 yeast and GGRBC particles in 1% OsO_4 (unbuffered or in PBSM) or in 1–5% glutaraldehyde in PBSM, were pipetted into the 600-μl capacity capsules. Each capsule was then filled by overlaying each sample with a 0.002% aqueous solution of BPB. The density difference between the sample suspensions and the BPB solution prevented mixing of the two layers. Filtration was initiated by touching a drop of 25% ethanol to the underside of each filter. Filtrate drops were collected in hollow polyethylene stoppers for inspection of filtrates by LM. As filtration proceeded, the BPB solution was carefully replenished in each capsule to maintain a small amount of hydrostatic pressure over the filters. Filtration was complete when the filtrate drop turned blue (usually 30–90 min, depending on the amount of sample applied). Each unit was then removed from the rack and placed on a glass plate in a small puddle of BPB solution (to exclude air from the bottom of the unit). A small amount of BPB solution was carefully added to the capsule to raise the level of the solution until the convex meniscus protruded above the capsule wall. A processing plug (filter end down) was wetted with BPB, inserted into the capsule (without trapping air), and slowly lowered until the covering filter approached the specimen layer, the BPB solution escaping up the lateral grooves in the sides of the processing plug (Fig. 1). The reverse taper of the capsule wall permitted the lower end of the processing plug to approach the sample layer without stressing the lower capsule wall (which would cause wrinkling of the specimen filter), while the slightly tighter fit at the upper end of the capsule provided enough friction to hold the processing plug securely in position (Fig. 1).

EMBEDDING, SECTIONING, AND STAINING: After insertion of the processing plug, each unit was returned to the rack, and the specimens were dehydrated in a graded series of ethanol solutions (50, 70, 95, 100, and 100%; 15 min each) which were placed in the center well of the processing plug (Fig. 1). The units were then transferred to no. 4 hollow polyethylene stoppers in which they were taken through 35% (vol/vol) propylene oxide in absolute ethanol (2 × 15 min), 1:1 (vol/vol) 35% propylene oxide: Epon 812 (30–60 min), and Epon (60–90 min). The Epon was then drained and replaced with enough fresh Epon to cover the filters in the vertically standing units (~2 ml/cup). The cups were then placed in a 60°C oven for at least 24 h to polymerize the resin. When hard, each embedded unit was removed from the cup and the upper part of the unit was cut off, giving a flat Epon disc which contained the lower part of the unit. The Epon discs were then trimmed to expose the sample layer and the two filters. Large silver-to-gold thin sections (1–2 mm × 0.2–0.5 mm) were cut perpendicular to the sample layer with a diamond knife (DuPont Instruments, Wilmington, Del.) on an LKB ultramicrotome (LKB Instruments, Inc., Rockville, Md.). The sections were picked up from below on parallel-bar grids, with the specimen layer running approximately perpendicular to the grid bars. Sections were stained with uranyl and lead salts as described previously (11).

COUNTING TECHNIQUE: Grids were examined in a Hitachi HU-11B electron microscope at 75 KV. Each grid was rapidly scanned to obtain orientation and to determine the condition of the thin sections. When a suitable series of section areas was selected for analysis, counting was begun at one end of the series (Fig. 2). Specimen profiles were examined through × 10 binoculars at an instrument magnification of × 1500. The frequencies of various profile types were tallied with manually operated counters. In control experiments, specimen profiles were scored simply as either yeast or GGRBC profiles. For assaying vacuole fusion, specimen profiles were classified into several types: (*a*) bare particle, a yeast or GGRBC profile not surrounded by a membrane profile (or only partially surrounded); (*b*) yeast vacuole (Yv), one or more yeast profiles completely surrounded by a single membrane profile; (*c*) GGRBC vacuole (Rv), one or more GGRBC profiles completely surrounded by a single membrane profile; and (*d*) hybrid vacuole (Hv), one or more yeast profiles

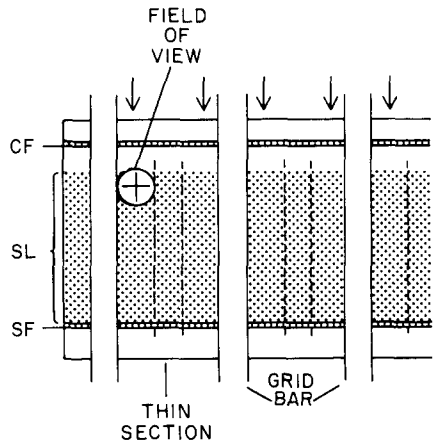

FIGURE 2 Schematic diagram of the technique used for obtaining data from ultrathin sections. Individual "counting strips" are indicated by the arrows. The approximate width of each strip extends from the edge of a grid bar to the edge of the field of view, indicated by the dashed lines. Specimen profiles within a strip were classified and tallied while scanning parallel to the grid bars. When a given strip was finished, counting was resumed at an adjacent strip. *CF*, covering filter; *SL*, specimen layer; *SF*, specimen filter.

and one or more GGRBC profiles completely surrounded by a single membrane profile. The total number of yeast and/or GGRBC profiles in a given class was also sometimes recorded. Because of the relative ease of scoring yeast profiles (vs. GGRBC profiles) (see reference 11), results were usually recorded relative to the yeast profile population. Vacuole concentrations were expressed either as relative percentages (e.g., no. Hv profiles/no. [Yv + Hv] profiles × 100), or as the apparent no. of vacuoles/ml (e.g., [no. Hv profiles/total no. yeast profiles] × no. yeast particles/ml). Typically, 1,000–2,000 counts were made per sample.

Light Microscopy

To examine the correlation of particle frequency data obtained by EM with that obtained by LM, test populations containing roughly 3, 9, and 15% yeast particles were prepared in separate test tubes by combining appropriate portions of yeast and GGRBC stock suspensions. Determination of the actual percentage of yeast particles in each of the three populations was then made by oil immersion phase contrast microscopy (slide and coverslip preparations). Five samples per population were counted, with 1,000 counts made per sample (100 counts at each of 10 different locations under the coverslip). An aliquot of each population was then prepared for EM analysis by the filtration technique (above) and the percentage of yeast profiles in each preparation was determined by use of the EM counting technique described above.

Total yeast and GGRBC particle concentrations in each of the cell homogenates were determined by hemocytometer counts (1:100 dilution with PBSM). The percentage of particles of a given type excluding eosin Y was routinely determined by diluting reaction mixtures from fusion experiments (already diluted 1:6 with DF) 1:7.7 with DDF, to give a final dye concentration of 0.30%. For each sample, a simple counting chamber was prepared on a clean glass slide by supporting a no. 1½ coverslip with two 1 × 1.5-cm Nuclepore filter strips (nominally 10 μm thick) that were spaced ~7 mm apart. A small aliquot (4–5 μl) of the dye-sample mixture was applied to the edge of the chamber and allowed to flow in by capillary action. Samples were observed under oil immersion (100 × objective) and the number of stained particles of a given type was determined by counting groups of 100 particles at different locations on the slide. Typically, 800–1,000 particles were counted per sample.

For assaying vacuole fusion by LM, reaction mixtures (already diluted 1:6 with DF) were diluted 1:11 with DDF and 4–5 μl of this mixture was added to a counting chamber as described above. The samples were observed under oil immersion and unstained yeast and GGRBC particles were classified by the following criteria. Two particles that were in the same focal plane were considered to be touching if oscillation of the fine focus of the objective by ~ ± 3 μm in sample depth would cause the optical boundary of one particle to be distorted by the optical boundary of the other. Two particles that were in slightly different focal planes were considered to be touching if, during oscillation of the fine focus, the superimposed particle images were judged to overlap by more than 50% of the image area of either particle. Two particles were considered to be in slightly different focal planes if the distance between the sharpest image of each was judged to be no greater than the thickness of a GGRBC particle (3 μm). If an unstained yeast or GGRBC particle appeared to be touching one or more unstained particles of the same type, the group was scored as a Yv or a Rv, respectively. If a group of unstained touching particles included both particle types, the group was scored as a Hv. In the many cases where the intravacuolar space was clearly delimited, the vacuole type was scored appropriately (even though the particles were not necessarily touching). Counts were usually done relative to the yeast population, to facilitate correlation with results obtained by EM (see above). LM results were expressed in essentially the same manner described for EM results (above). Typically, 600 vacuoles were classified per sample, counting in groups of 100 at six different locations on the slide. Photomicrographs were made as previously described (11).

RESULTS

General Appearance of EM Specimens

Ideally, it is desired to prepare a perfectly even layer of particles and to process and embed the

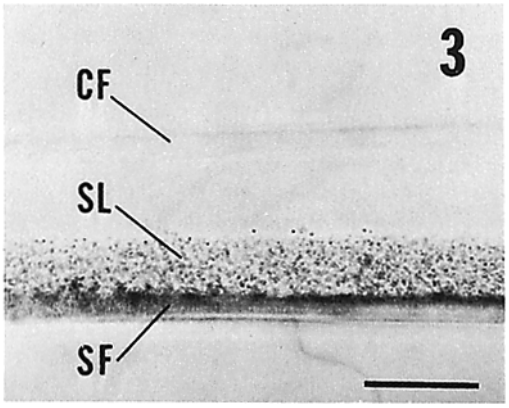

FIGURE 3 Light micrograph of a typical region within an Epon-embedded specimen layer prepared by the filtration technique (1% OsO_4 fixation). A thick section (about 30 μm thick) was cut perpendicularly to the specimen layer, placed in immersion oil between a slide and coverslip, and photographed with phase contrast optics. The specimen layer (*SL*) is seen to be of uniform thickness. *CF*, covering filter; *SF*, specimen filter. Bar, 100 μm. × 150.

layer without disturbance (see Discussion). While some imperfections in the preservation of the specimen pellicles prepared by the filtration technique were usually observed, in general, the pellicles were found to be reasonably uniform. A cross section of a typical region within such a pellicle is shown at low magnification in Fig. 3. An electron microscope view of a cross section through a similar pellicle is shown in Fig. 4. Optimal preservation of pellicle structure was obtained with direct osmic acid fixation. Pellicles fixed with glutaraldehyde usually showed horizontal shifting of portions of the pellicle during processing. On the other hand, the more brittle and generally quite uniform osmium-fixed pellicles (e.g., Fig. 3), often showed a dislocation or fracture at one or more locations within the pellicle. Wrinkling of the specimen filter appeared to be the main cause of such imperfections (see Discussion). However,

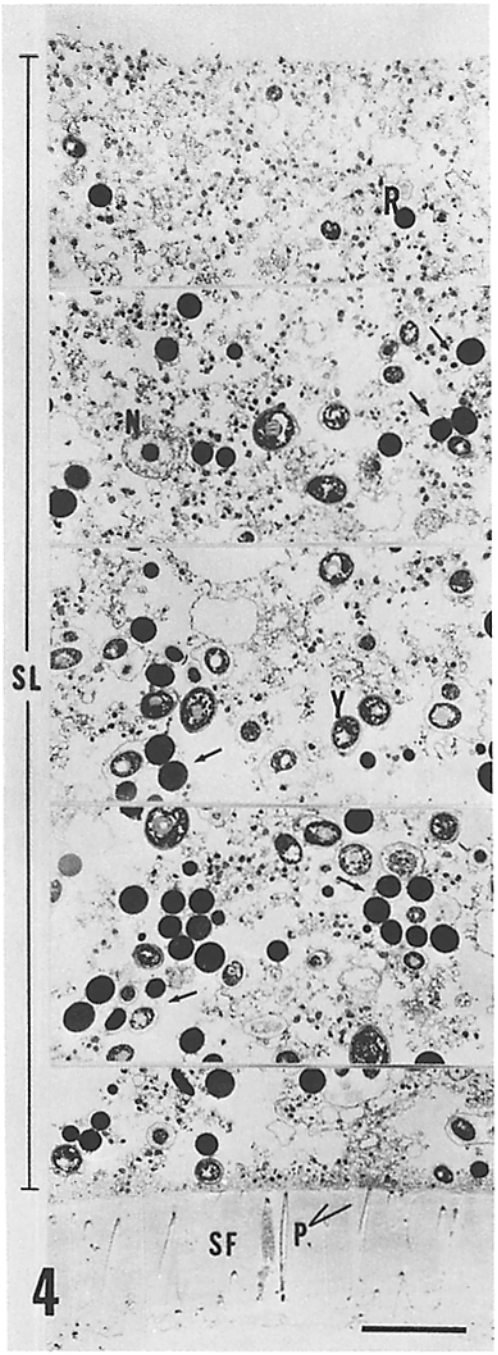

FIGURE 4 A series of electron micrographs encompassing a typical region of a specimen layer prepared from an in vitro fusion incubation mixture by the filtration technique. To be manageable for the purposes of reproduction, the apparent thickness of the specimen layer was reduced by 40% by omitting ~18 μm of the layer between each micrograph shown. The fields show slight distortion due to the low magnification at which the micrographs were taken. Hybrid vacuoles containing yeast and GGRBC particles are indicated by the arrows. It should be noted that EM counting was done at a magnification ~× 10 higher than that of this figure. *R*, GGRBC particle; *Y*, yeast particle; *N*, cell nucleus; *SL*, specimen layer; *SF*, specimen filter; *P*, filter pores. Bar, ~10 μm. ~× 1400.

partly because of the use of the two-dimensional counting technique (Fig. 2), the distortions which were observed proved to be of negligible consequence. Compared with pellicles prepared by the filtration technique, pellicles prepared by the sedimentation technique were generally of equal or better uniformity.

Quantitative EM Control Experiments

Before attempting to obtain data on the in vitro PL fusion reaction by EM counts of specimens prepared by the filtration technique, control experiments were performed to assess the reproducibility and reliability of data obtained by this method. To test the reproducibility of the procedure, triplicate samples of a homogenate mixture from a fusion experiment were independently prepared by the filtration technique, and the percentage of yeast profiles relative to the total population of yeast and GGRBC profiles was determined by EM counts of each of the three samples. The results were quite consistent: 46.4 ± 0.8% yeast profiles (mean ± SD; 1,200–1,600 profiles counted/sample). Similar consistency was obtained when individual specimen pellicles were sectioned at different locations within the pellicle (data not shown). In an experiment to test the reliability of such results, three mixtures of yeast and GGRBC particles, each of a different relative composition, were prepared as test populations, and the percentage of yeast was determined in each of these populations by both LM (% yeast particles) and by EM (% yeast profiles). As is evident in Table I, the results obtained by EM were indistinguishable from those obtained by LM. Similar results have been obtained with specimens prepared by the more recent sedimentation method. These results demonstrate that, using the techniques described, accurate and reproducible particle frequency data concerning these types of particle populations can be obtained directly from ultrathin sections.

TABLE I

Percentages of Yeast as Determined by LM and EM

Particle mixture no.	Light microscopy	Electron microscopy	
	Yeast particles*	Yeast profiles/ total count	Yeast profiles‡
	avg %		%
1	3.7 ± 0.3	80/2,127	3.8
2	9.3 ± 0.8	211/2,268	9.3
3	17.1 ± 1.1	377/2,168	17.4

* Mean ± SD. Five samples/mixture, 1,000 particles counted/sample.

‡ One sample/mixture.

Quantitation of PL Fusion by EM

The techniques described above were then applied to the measurement of in vitro PL fusion. A quantitative electron microscope analysis of the time course of a typical fusion reaction is shown in Fig. 5. The levels of membrane-bounded GGRBC particles (Riv) and of membrane-bounded yeast particles (Yiv) are seen to remain constant throughout the course of the incubation (Fig. 5*a*). During the same incubation, the apparent concen-

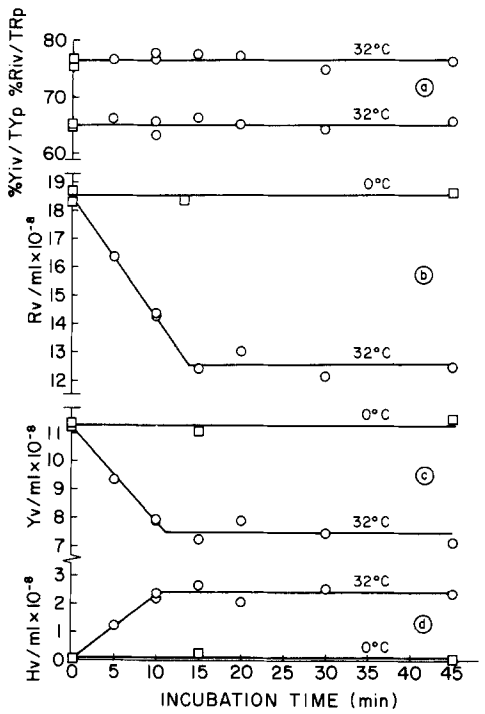

FIGURE 5 The time and temperature dependence of a typical in vitro PL fusion reaction, as determined by EM. The levels of membrane-bounded GGRBC profiles (*Riv*) and membrane-bounded yeast profiles (*Yiv*) are plotted as a function of in vitro incubation time in Fig. 5*a*. The apparent concentrations of vacuoles containing only GGRBC particles (*Rv*), of vacuoles containing only yeast particles (*Yv*), and of vacuoles containing both GGRBC and yeast particles (*Hv*) are plotted as a function of in vitro incubation time and temperature in Figs. 5*b*, 5*c*, and 5*d*, respectively. Profile counts of *Rv*, *Yv*, and *Hv* were converted into the apparent no./ml of each vacuole type by the means described in Materials and Methods. *TRp*, total GGRBC profiles; *TYp*, total yeast profiles.

TABLE II

The Effects of Several Metabolic Inhibitors on PL Fusion In Vitro (EM)

Sample no.	Incubation time	Additions	Total count*	Yeast vacuoles (Yv)	Hybrid vacuoles (Hv)	Total vacuoles (Yv + Hv)	Hybrid of total vacuoles
				%	%	%	%
1	0′	–	1,444	54.8	0.07	54.9	0.1
2	10′	–	1,292	48.6	9.4	58.0	16.2
3	10′	–	817	45.8	9.8	55.6	17.6
4	10′	8 mM KCl	1,230	47.0	10.7	57.7	18.5
5	10′	1 mM KCN	1,014	44.8	9.3	54.1	17.2
6	10′	4 mM KCN	1,210	42.7	8.9	51.6	17.2
7	10′	0.1 mM 2,4-DNP	1,117	42.0	7.9	49.9	15.8
8	10′	4 mM KF	1,344	51.1	4.2	55.3	7.6
9	10′	4 mM KF + 4 mM KCN	1,508	46.9	3.4	50.3	6.8
10	10′	4 mM KF + 4 mM KCN + 0.05 mM 2,4-DNP	1,647	43.8	2.3	46.1	5.0

* EM counts of the yeast population (only). The total count is the sum of the number of bare yeast, Yv, and Hv scored in each sample (see Materials and Methods).

trations[4] of Rv and Yv (Figs. 5*b* and 5*c*, respectively) are seen to decrease linearly, in a temperature dependent manner, for an initial 10–15 min, after which the levels remain constant. At the same time, the concentration of vacuoles containing both GGRBC and yeast particles (Hv) (Fig. 5*d*) is seen to increase in a manner that is temperature dependent and that mirrors the Rv and Yv patterns, the Hv concentration increasing linearly for 10 min, and then remaining constant. Consistent with the finding that the total number of membrane-bounded particles of both types remains constant during the incubation (Fig. 5*a*), while the total number of vacuoles (Rv + Yv + Hv) simultaneously decreases (Figs. 5*b*, 5*c*, and 5*d*), it was observed that the size and frequency of multi-particle vacuoles increased significantly during the incubation. For example, while the great majority of vacuole profiles in unincubated mixtures contained only a single particle profile, vacuole profiles in mixtures that had been incubated at 30–32°C were frequently observed to contain five or more particle profiles (e.g., see Fig. 4). The relative magnitudes of the changes in vacuole concentrations ($\Delta Rv > \Delta Yv > \Delta Hv$) (Figs. 5*b*, 5*c*, and 5*d*) should also be noted, as they are consistent with fusion occurring among the reacting vacuoles in a random manner (see below). It should also be mentioned that, as observed previously (11), vacuoles were seen to have fused only with other vacuoles. Fusion of other classes of subcellular organelles (e.g., mitochondria and nuclei), either with other members of the same class or with members of different classes, was not detected.

The effects of several metabolic inhibitors on the PL fusion reaction were also examined. In early semiquantitative studies, it was observed that the PL fusion reaction appeared to be strongly inhibited by the combined presence of KF, KCN, and 2,4-dinitrophenol (2,4-DNP) in the incubation mixtures. Quantitative experiments were therefore carried out to confirm and further define the effects of these compounds on the fusion reaction. EM data obtained from such an experiment are tabulated in Table II. In confirmation of the earlier results, a marked reduction

[4] These concentrations are apparent since, because of their sectioning orientation, some percentage of hybrid vacuoles will be detected in the thin sections as being simply Rv or Yv. This results in a slight overestimation of the true Rv and Yv levels, and an underestimation of the true Hv levels. While mathematical derivation of the necessary corrections for sectioning would be quite complicated (being a function of the number, size, shape, orientation, and particle composition of the hybrids in each sample, among other factors), these corrections can be estimated from a comparison of EM data with data derived from a three-dimensional analysis of the same samples by LM (see text). By this method, the underestimation of the Hv concentration in samples incubated for 10 min or longer at 32°C in Fig. 5 was found to average <25%. With the assumption that in the EM analysis, half of the "missed" hybrids were scored as Rv, and half as Yv, the overestimations of the true Rv and Yv concentrations in Fig. 5 averaged less than <3 and 6%, respectively. See text for further discussion.

in the hybrid vacuole level was found when the incubation was carried out in the presence of KF, KCN, and 2,4-DNP (Table II, sample 10). Furthermore, the effect was seen to be largely attributable to fluoride, since KCN alone and 2,4-DNP alone had little or no effect (samples 5–7), while KF alone, or in combination with KCN (samples 8 and 9), produced a reduction in the hybrid levels comparable to the combination of the three inhibitors (sample 10). That the action of KF was not simply a result of a nonspecific salt effect is evidenced by the lack of effect of KCl (sample 4), which was added to the incubation mixture at twice the concentration used for KF. It should be noted that KF (at the concentration shown) had no effect on the total vacuole level (sample 8 vs. samples 1–3). These results were fully supported by data obtained by LM (below).

Quantitation of Vacuole Levels by LM

Once some of the basic properties of the in vitro vacuole fusion reaction were defined by EM, efforts were made to develop a faster method of analysis.

Based on the previously reported observation that *Acanthamoeba* phagolysosomes were transiently capable of excluding eosin Y (11), a light microscope assay was developed for measuring the concentrations of yeast- and GGRBC-containing vacuoles (as well as the number of particles within such vacuoles).[5] A portion of a typical light microscope field of vacuoles and particles is shown in Fig. 6. A key feature of the light microscope assay is the use of DDF, which is composed mainly of filtered *Acanthamoeba* cytoplasm (DF). Of various media tested, this preparation was the only one with which (*a*) dye exclusion values were maximal, and (*b*) dye exclusion values remained constant during the counting procedure (20–40 min/sample). With this reagent, the percentage of unstained yeast and/or GGRBC particles in a given preparation was found to be independent of the dye concentration employed, up to a concentration of 0.7% (data not shown). Above this concentration, a progressive leakage of the dye into the vacuoles was detected during the counting. At a constant dye concentration, the percentage of unstained yeast and/or GGRBC particles in a given preparation was also found to be independent of the extent of dilution with DDF, at all dilutions tested (data not shown). Since previous evidence indicates that the property of dye exclusion by these particles depends on the presence of an undamaged vacuolar membrane (11), these data indicate that at least a constant fraction of the vacuolar membranes in a given preparation is stable to the handling and testing conditions involved in the dye exclusion test. To answer the questions of (*a*) whether a significant fraction of the vacuole populations might be "leaky" due to damage suffered during the hypotonic swelling and the homogenization steps, and (*b*) whether the procedures employed might cause some "fragile" subpopulation of vacuoles to be consistently ruptured or damaged before the counting step, values obtained by the dye exclusion test were compared with results obtained for the same samples by EM (Table III). As can be seen in Table III, values obtained by the two methods closely agreed. These results show that under the conditions described, the presence of a vacuolar membrane around the marker particles can be detected by LM with the same accuracy and reliability as by EM.

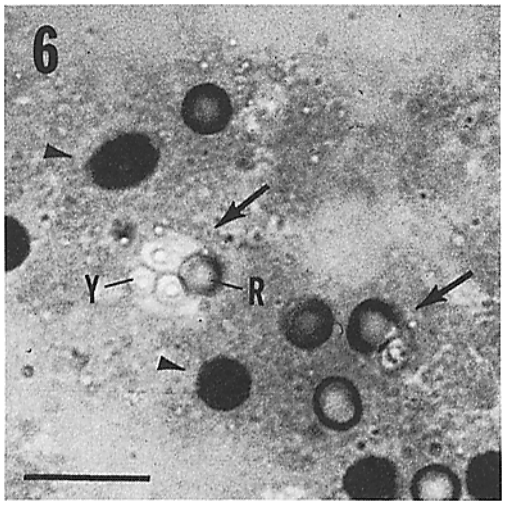

FIGURE 6 Light micrograph of a portion of an in vitro reaction mixture that has been diluted with DDF. Two apparent hybrid vacuoles are indicated by the arrows. In contrast to the intensely stained particles nearby (arrowheads), the yeast (*Y*) and GGRBC (*R*) particles within these vacuoles are seen to be unstained. Black and white print of a color photograph. Bar, 10 μm. Bright field. × 1,600.

[5] Since there was always a certain percentage of vacuoles which contained more than one particle, the concentration of vacuoles was always somewhat less than the concentration of membrane-bound particles. Depending on the nature of the experiment, either one or both of these parameters were measured.

TABLE III

Particle Dye Exclusion (LM) vs. Membrane-Bounded Particle Profiles (EM)

Exp no.	Particle type	Light microscopy: Unstained particles	Electron microscopy: Membrane-bounded particle profiles
		%	%
1	Yeast	69.4 ± 1.2* (5)	69.0 ± 2.0 (3)
2a	Yeast	67.0 ± 1.2 (4)	65.0 ± 1.1 (11)
2b	GGRBC	75.6 ± 3.6 (3)	75.8 ± 2.1 (11)

* Mean ± SD. The number of determinations is shown in parentheses. LM: 600–800 particles counted/sample; EM: 1,300–1,400/sample.

Quantitation of PL Fusion by LM

PL fusion in vitro was routinely monitored by measuring the levels of hybrid vacuoles produced by the incubation of mixtures of Rv- and Yv-containing homogenates at 30–32°C. While it should be borne in mind that distinct boundaries do not exist between the following classes, it is nevertheless useful for the present purposes to define two general morphological classes of hybrid vacuoles: a "loose" class, in which the vacuolar membrane quite loosely surrounds the marker particles (e.g., Fig. 7a), and a "tight" class, in which the vacuolar membrane tightly surrounds the particles (e.g., Fig. 7b). Under appropriate conditions, hybrids of the "loose" class could clearly be discerned by LM (e.g., Fig. 6). However, hybrids of the "tight" class appear by LM simply as nonstaining marker particles of different types that are closely associated; the light microscope image is of insufficient resolution to determine the nature of the "close association," i.e., whether it is due to random juxtaposition of the vacuoles on the slide, to fusion of the vacuoles (Fig. 7b), or to adhesion of the vacuoles (Figs. 7c and 7d). Random juxtaposition of the vacuoles was reduced to negligible levels by diluting the vacuole suspension appropriately. A typical plot of dilution vs. the percentage of vacuoles scored by LM as hybrids (by the criteria defined in Materials and Methods) is shown in Fig. 8. It can be seen that a constant percentage of vacuoles were identified as hybrids at dilutions greater than about 1:50 under standard conditions. The persistent association of marker particles with "tight" morphologies at the dilution routinely employed (1:66) is thus either a result of vacuole adhesion or of vacuole fusion. To address the question of whether or not a significant percentage of this "tight" class was a result of adhesion, data obtained by the LM assay were compared with data obtained on the same samples by the EM assay (Fig. 9). As can be seen, the reaction pattern determined by the LM assay was quite similar to that obtained by the EM assay. Furthermore, the two methods yielded similar plateau values, the EM value being 15% lower than the LM value (Fig. 9, "32°C", $t > 10$ min). While exact calculation on this point is difficult, it is quite likely that this difference is entirely attributable to the lower efficiency of hybrid detection by EM as compared with LM, since some percentage of hybrid vacuoles will necessarily be missed in thin-sectioning, appearing to be either simply Rv or Yv (see Discussion). These data therefore indicate that in samples incubated at 32°C, "close association" of unstained particles as detected in the LM assay is a result of vacuole fusion; vacuole adhesion appears to be nonexistent or negligible in such samples.

Light microscope analyses of the Rv, Yv, and Hv reaction patterns yielded results that were quite similar to those found by EM (e.g., Fig. 5). As before, during incubation at 30–32°C, both the Rv and Yv populations decreased linearly and leveled off after 10 min, while the Hv population increased linearly and plateaued at about 10 min (data not shown). LM measurements also consistently confirmed the EM finding (Fig. 5a) that the levels of membrane-bounded yeast and GGRBC particles remain constant during the course of the in vitro incubation (data not shown).

Magnitudes of the Changes in Vacuole Concentration During Fusion

Data summarizing the results obtained from analyses of three in vitro fusion experiments are shown in Table IV. These data show that after incubation for 10 min at 30–32°C, the Rv and Yv concentrations decreased an average of 20 and 23%, respectively, while the Hv concentration increased an average of fourfold. It should be noted that, in each experiment, ΔRv and ΔYv were found to be greater than ΔHv. In addition, when the initial concentration of Rv (Rv_0) was equal to the initial concentration of Yv (Yv_0), ΔRv was equal to ΔYv (Table IV, exp 1). On the

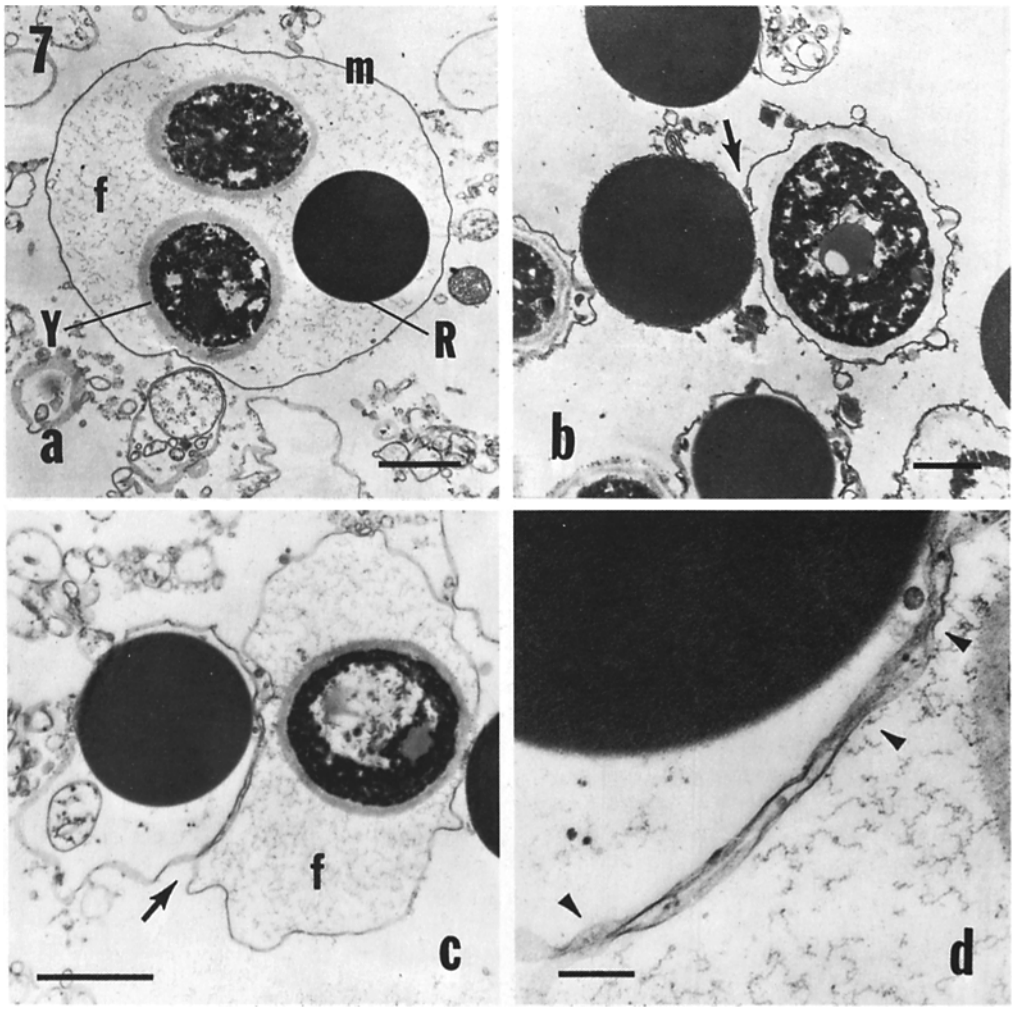

FIGURE 7 Several types of vacuole morphologies observed by EM. Fig. 7*a* shows a typical hybrid vacuole of the "loose" type, where the vacuole membrane (*m*) loosely surrounds the yeast (*Y*) and GGRBC (*R*) marker particles (cf. Fig. 6). Note the homogeneous intravacuolar distribution of the flocculent material (*f*). Fig. 7*b* illustrates a hybrid vacuole of "tight" morphology, where the vacuole membrane closely surrounds the two marker particles. The region of fusion between the two vacuoles is indicated by the arrow. In Fig. 7*c*, the membranes of two vacuoles are seen to be closely associated (arrow). The lack of homogeneity in the distribution of the flocculent material (*f*) between the two vacuoles suggests that free diffusion of the vacuolar contents between the two is impeded (cf. Fig. 7*a*). A higher magnification view of the region of apposition in Fig. 7*c* is shown in Fig. 7*d*. No open connections between the two membranes are evident, while adhesion between the two is suggested at several points (arrowheads). Such images were observed in significant frequencies only in samples which had not been warmed up to incubation temperature (30–32°C). See text for discussion. Bar, 0.2 μm. (*a*) × 11,000; (b) × 8,800; (*c*) × 15,000; bars, 1 μm. (*d*) × 51,000.

other hand, when Rv_0 was greater than Yv_0, ΔRv was greater than ΔYv (Table IV, exps 2 and 3). Finally, in each case, evaluation of the quantity $\Delta Hv/(\Delta Rv + \Delta Yv)$ gave a value of 0.3 (Table IV). In other words, despite different initial Rv/Yv ratios, and despite different absolute magnitudes of ΔRv, ΔYv, and ΔHv, ~1 concentration unit of hybrid vacuoles is produced for every 3 concentration units of Rv and Yv expended.

The above observations were found to be quan-

titatively consistent with the predictions of a simple model based on random fusion of Rv and Yv vacuoles (see Discussion).

Effects of KCl, KF, and 2,4-DNP on PL Fusion (LM)

To confirm and extend previous EM findings (e.g., Table II), and to test the correlation between the LM and the EM assays when the reaction conditions were experimentally perturbed, the effects of various concentrations of KCl, KF, and 2,4-DNP on the fusion reaction were examined by the LM assay. Due to the difficulties of maintaining known concentrations of cyanide in experimental mixtures (13), further experiments with KCN were not pursued.

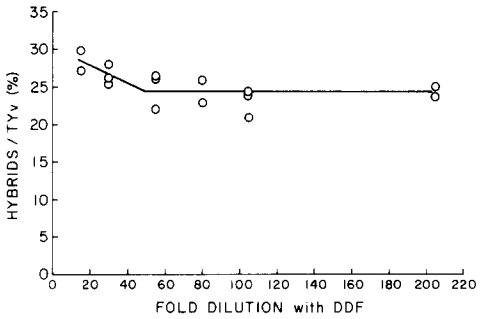

FIGURE 8 A typical plot of the dilution of a postincubation sample from an in vitro fusion reaction vs. the percentage of yeast-containing vacuoles that were scored as hybrids by LM. The slight rise in the curve at dilutions below 40-fold is due to random juxtaposition of yeast- and GGRBC-containing vacuoles (see text). At dilutions greater than 50-fold, the constancy of the hybrid level indicates that the nonstaining yeast and GGRBC particle combinations that are scored as hybrids are stably associated. *TYv*, total yeast-containing vacuoles (yeast vacuoles + hybrid vacuoles).

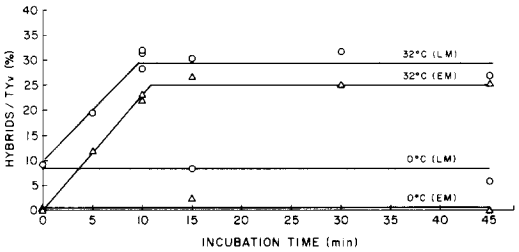

FIGURE 9 A comparison of in vitro reaction patterns for hybrid vacuole formation as measured by the LM assay and by the EM assay. Samples from an in vitro fusion reaction were analyzed for hybrid levels by LM, and then the same samples were analyzed for hybrids by EM. Ordinate: the percentage of apparent hybrid vacuoles (by LM) or hybrid vacuole profiles (by EM) relative to *TYv*, the total number of apparent yeast-containing vacuoles (LM) or yeast-containing vacuole profiles (EM).

Results of a series of experiments in which varying amounts of KCl were added to the homogenates before the incubation are shown in Fig. 10. In agreement with earlier EM results, it was found that the fusion reaction was unaffected by low concentrations of KCl (8 mM), but was increasingly inhibited by added KCl concentrations >10 mM, with complete suppression of the reaction occurring between 45 and 90 mM (Fig. 10b). 50% inhibition was observed at ~25 mM. Up to 30 mM of added KCl (where the reaction was inhibited some 60%), no change in the integrity of the vacuolar membranes was detected by the dye exclusion criterion (Fig. 10a). However, at

TABLE IV

Changes in Vacuole Concentrations during the In Vitro Incubation

Exp no.	Assay method	Rv_0*	Yv_0	Hv_0	ΔRv	ΔYv	ΔHv	$\frac{\Delta Hv}{\Delta Rv + \Delta Yv}$
		$\times 10^{-8}$/ml						
1	LM	10.03 ± .01‡ (2)	10.09 ± .13 (2)	0.32 ± .06 (2)	1.50 ± .14 (2)	1.57 ± .18 (2)	1.00 ± .06 (2)	0.33 ± .03
2	LM	13.72 ± .04 (3)	9.17 ± .32 (3)	0.48 ± .03 (3)	2.80 ± .06 (2)	2.03 ± .32 (2)	1.43 ± .07 (2)	0.30 ± .03
3	EM§	18.13 ± .42 (3)	10.93 ± .08 (3)	0.90 ± .58 (3)	4.26 ± .42 (2)	3.44 ± .08 (2)	2.40 ± .58 (2)	0.31 ± .08

* Rv_0, Yv_0, and Hv_0 are the respective concentrations of GGRBC-containing vacuoles (Rv), yeast-containing vacuoles (Yv), and GGRBC- and yeast-containing vacuoles (Hv) in homogenate mixtures that were incubated on ice. ΔRv and ΔYv are the decreases in the Rv and Yv concentrations (e.g., $\Delta Rv = Rv_0 - Rv[t]$), and ΔHv is the increase in the Hv concentration (i.e., $\Delta Hv = Hv[t] - Hv_0$), which occurred after incubation of the mixtures at 30–32°C for t = 10 min.

‡ SD. The number of determinations is shown in parentheses. ~1,000 vacuoles were counted per determination.

§ The Hv values are corrected for underestimation as a result of sectioning, calculated from data for this experiment shown in Fig. 9, assuming that the difference between the LM and EM curves in Fig. 9 is entirely a result of sectioning loss. Likewise, the Rv and Yv data are corrected for slight overestimation resulting from the same cause (see footnote 4).

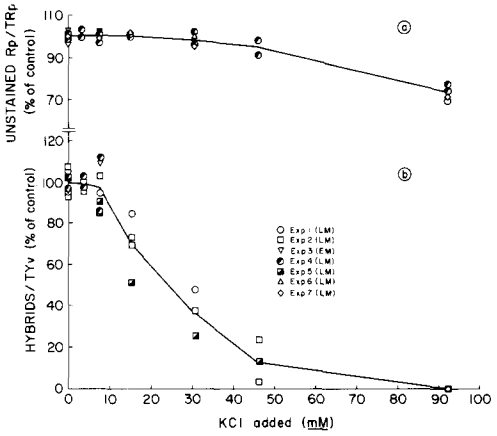

FIGURE 10 The effects of KCl on the in vitro formation of hybrid vacuoles. All samples were incubated for 10 min at 30–32°C. In each experiment, the average control value (no KCl added) was taken as 100%. After incubation, the effects of KCl on vacuole membrane integrity was measured by dye exclusion (10*a*). Hybrid vacuole levels are plotted in Fig. 10*b*. *Rp*, GGRBC particles; *TRp*, total GGRBC particles; *TYv*, total yeast-containing vacuoles.

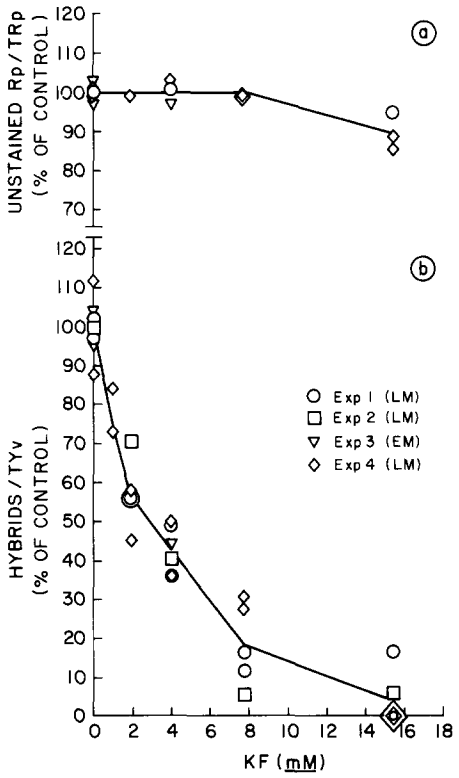

FIGURE 11 The effects of KF on the in vitro formation of hybrid vacuoles. All samples were incubated for 10 min at 30–32°C. In each experiment, the average control value (no KF added) was taken as 100%. Postincubation dye exclusion values are shown in Fig. 11*a*, and hybrid levels are plotted in Fig. 11*b*. Note the different scale of the abscissa compared with Fig. 10. *Rp*, GGRBC particles; *TRp*, total GGRBC particles; *TYv*, total yeast-containing vacuoles.

added KCl concentration >30 mM, increasing dye uptake by the vacuoles was observed (Fig. 10 a).

In contrast to these results, the fusion reaction was observed to be approximately an order of magnitude more sensitive to KF, with 50% inhibition of the reaction occurring at ~2.7 mM (Fig. 11 b). Vacuole integrity as measured by dye exclusion was unaffected by KF concentrations up to 8 mM (where the reaction was inhibited >80%) (Fig. 11 a). At 15 mM KF, an increase in particle staining of ~10% was detected (Fig. 11 a). It should be noted that the LM results were quantitatively consistent with previous EM data. For example, the inhibition by 4 mM KF in the three LM experiments shown in Fig. 11 b was 58 ± 7% (mean ± SD); the inhibition by 4 mM KF in the experiment shown in Table II (calculated from samples 1, 2, 3, and 8) is 55% (also plotted in Fig. 11 b).

Concentrations of 2,4-DNP ranging from 10 up to 200 μM were found to have little effect on the PL fusion reaction (data not shown). Again, the results obtained by the LM assay were found to be quantitatively consistent with previous results obtained by the EM assay. For example, in three experiments done by LM, hybrid levels obtained in the presence of 100 μM 2,4-DNP were an average of 92 ± 3% (SD) of the control values. The corresponding value obtained by EM in Table II (from samples 1, 2, 3, and 7) is 94%.

DISCUSSION

Development of the EM Assay

To define the properties of the PL fusion reaction, it was necessary to develop a reliable method for measuring PL fusion. An obvious requirement for such a method is that it measure vacuole fusion, as opposed to vacuole adhesion or aggregation. Of various methodological approaches that were considered, thin section EM was judged to be the most reliable; although it would always yield an underestimation of the true hybrid levels due to sectioning losses, in principle it would be

least susceptible to giving falsely positive or erratic results as reaction conditions were experimentally varied. However, early attempts to employ EM for this purpose were frustrated by the problem of nonrandom sampling, a consequence of the conventional EM preparative methods that were employed (2, 15). Although this problem could be largely overcome by the use of a two-dimensional scanning procedure (11), the heterogeneity of the particle distribution within the specimen pellets frequently necessitated laborious resectioning and counting of additional specimen areas to obtain a total sampling that was representative enough to give reasonably consistent numerical values. Even then, the precision of the method was not very high (11).

Attention was therefore turned to developing a simple method for preparing the specimens as thin pellicles which were heterogeneous solely in the vertical dimension, so that a thin section from the top to the bottom of the pellicle would provide a truly representative sample of the specimen (1, 9, 15, 18). In agreement with observations of Baudhuin et al. (1), and of Worsfold et al. (18), our early experience showed that it was necessary to protect such pellicles from erosion caused by the numerous solution changes during the embedding procedure. A technique similar in principle to that of Worsfold et al., which is a modification of that of Baudhuin et al., was therefore developed. In the present case, because of the relatively large size of the particles under study (>1 μm diameter), and of the use of Nuclepore filters, the complexity of the filtration unit could be considerably reduced, since adequate filtration was found to occur through the 0.8 μm-pore filters without the need of an external pressure source. The employment of Nuclepore filters also allowed the "filter sandwich" to be directly embedded in Epon 812 (cf. references 1, 18). However, it was found necessary to use propylene oxide at a reduced concentration (35% [vol/vol] in absolute ethanol), since propylene oxide at full strength (8) caused the epoxy-mounted filters to tear (from becoming extremely taut). On the other hand, omission of propylene oxide resulted in Epon embeddings that failed to fully polymerize in the immediate vicinity of the fixative-treated specimen filter. Use of propylene oxide at 35% was therefore an empirically determined compromise in which the propylene oxide concentration was low enough to cause only a slight increase in filter tautness, and yet was high enough to allow satisfactory hardening of the embeddings, usually by 72 h at 60°C, although some specimens were sectionable after 24 h. Such problems were not encountered with the newer sedimentation technique (10).

Development of the LM Assay

EM was initially employed to characterize the fusion reaction to ensure that fusion, and not aggregation or adhesion, was being measured. While the distinctive advantage of EM is its high resolution, its inherent disadvantage is the relative slowness of the preparative techniques required. Therefore, once the basic characteristics of the reaction were delineated by EM, efforts were made to develop a faster assay by LM, particularly one that would avoid the time-consuming procedures of fixation, dehydration, embedding, and sectioning. The major barrier to developing the LM assay described here was the instability of the vacuoles on the light microscope stage (see reference 11). Oil immersion microscopy was necessary to allow accurate identification of the two particle types, but standard slide and coverslip preparations were unsatisfactory, because settling of the coverslip damaged the vacuoles. On the other hand, standard counting chambers for cells or bacteria are too thick for oil immersion work. Mounting of coverslips on small strips of Nuclepore filters (nominally 10 μm thick) was found to be a satisfactory solution to this problem.

It was also found necessary to develop a medium in which the vacuoles would be stable on the light microscope stage in the presence of the dye. Of various media tested for this purpose, the most satisfactory was filtered *Acanthamoeba* cytoplasm, prepared as described in Materials and Methods. Employment of this medium resulted from the somewhat surprising observation that the vacuoles appeared to be quite stable to dye penetration for long periods of time (>1 h) when they were examined in homogenates that were virtually undiluted. Although the reason why this is so is not clear at present, the effectiveness of this preparation in yielding counts of vacuoles that are both consistent and accurate is evidenced by the results obtained with it (e.g., Table III).

Assay of PL Fusion by LM and EM

It should be emphasized that the appearance of a hybrid vacuole by LM is, in many cases,

unambiguous (e.g., Fig. 6). However, since in a significant number of cases, the LM image is ambiguous, it was necessary to develop objective criteria for identifying hybrids by LM. While some of the criteria employed were necessarily somewhat arbitrary (see Materials and Methods), they were derived from a great many EM observations of hybrid morphology. Their effectiveness is evidenced by, in all cases to date, results obtained by LM, which have been in close agreement with those obtained by EM (e.g., Figs. 9 and 11). As expected, the actual values obtained for hybrid levels were always found to be lower by EM than by LM. The magnitudes of the differences between the two methods (e.g., Fig. 9) are consistent with the lower efficiency of hybrid detection by EM expected from sectioning. The larger sized hybrids formed as the reaction progresses will have an increased probability of being detected in thin sections as hybrids. Thus, the difference between the LM and EM values is expected (*a*) to be maximal and constant in samples kept at 0°C, (*b*) to decrease as the reaction progresses, and (*c*) to be minimal and constant when the reaction plateaus (Fig. 9).

Comment should be made on the results for samples kept at 0°C. That images such as shown in Fig. 7 c were observed in significant frequency only in samples incubated at 0°C, suggests that the association observed is not an artifact of the EM preparative procedure (since all of the samples were prepared in the same way). Fusion in such samples is presumably a result of the brief warming of the cold reaction mixtures when they are pipetted in room temperature micropipettes before the addition of the stopping reagent. LM observations show that the apparent hybrids in such samples are almost all of the "tight" morphology, consisting typically of a single nonstaining GGRBC particle in close association with a single nonstaining yeast particle. If it is hypothesized that the brief warming of the "0°C" samples allowed only the initial steps of fusion to occur, i.e., the formation of a very short, narrow diameter "fusion channel" (see reference 11), then, besides greatly lowering the efficiency of hybrid detection in thin sections, such a morphology would also be consistent with Fig. 7 c. While such channels were not noted during the EM counts of these samples, such channels would be expected to be only rarely visible in thin sections, and, if occasionally present, could have been overlooked at the, relatively, low counting magnification employed. Thus, while part of the difference between the LM and EM values for the 0°C samples may be a result of vacuole adhesion as suggested by Fig. 7 c (i.e., overestimation of hybrids by LM in addition to a relatively large underestimation expected by EM), it should be noted that such images are not necessarily inconsistent with true fusion. Further study will be necessary to resolve this point.

In any event, it can be concluded that although some degree of vacuole adhesion may occur in samples incubated at 0°C, the LM assay is as reliable as the EM assay for measuring hybrid vacuole levels in samples which have been incubated at 30–32°C, under all of the conditions we have thus far tested. It should be emphasized, however, that since the conditions under which vacuole adhesion may be induced (e.g., reference 14) are presently undefined in this system, caution is necessary in applying the LM assay to new experimental conditions. Once the absence of adhesion under a given set of conditions is established by EM, the LM assay allows routine, relatively rapid, and three-dimensional analyses of the vacuole populations, which is not possible by EM. In addition, the LM assay has the potential for even greater efficiency, since it appears to be readily adaptable to the use of automated image analysis techniques.

Characteristics of the In Vitro Reaction Process

If vacuole fusion is in fact the mechanism by which hybrid vacuoles are formed during the in vitro incubation (11), then it follows that the concentrations of nonhybrid vacuoles should decrease during hybrid formation. Previous electron microscope analysis of conventionally embedded samples failed, however, to detect any change in the nonhybrid (Yv) concentration during hybrid formation (see Fig. 14 in reference 11). This discrepancy was interpreted as a result of the relatively low levels of hybrids produced and of the relative imprecision of the analytical technique employed (11). The present results, obtained with improved analytical methods and with an improved in vitro system (higher vacuole levels and higher hybrid levels), confirm the previous interpretation and clearly demonstrate the kinetic relationships between the three vacuole populations (e.g., Fig. 5). The present findings that (*a*) the total number of membrane-bounded yeast and GGRBC particles remains

constant (e.g., Fig. 5 a), while (*b*) the Rv and Yv concentrations simultaneously decrease (e.g., Figs. 5 b and 5 c), while (*c*) the Hv concentration simultaneously increases (e.g., Fig. 5 d), and (*d*) the concentration changes in each of the three populations synchronously cease at 10–15 min (e.g., Figs. 5 b, 5 c, and 5 d), together clearly demonstrate that the formation of hybrid vacuoles is tightly coupled to a nondestructive expenditure of yeast- and GGRBC-containing vacuoles. The only plausible interpretation of these results is that the vacuoles are fusing.

The present results also indicate that vacuole fusion occurs in an essentially random manner with respect to vacuole type. This interpretation is consistent with previous evidence which indicated that fusion per se was independent of the type of particle within the vacuoles (11). The data concerning the relationships between ΔRv, ΔYv, and ΔHv in Table IV were found to be consistent with the following relationships derived from a simple model that postulates random fusion of the vacuoles (see Appendix):

$$\Delta Rv = ([Rv_0/2Yv_0] + 1)\Delta Hv \quad (1)$$

$$\Delta Yv = ([Yv_0/2Rv_0] + 1)\Delta Hv. \quad (2)$$

It can be seen that since Rv_0 and Yv_0 are nonzero, ΔRv and ΔYv in Eqs. 1 and 2 will always be greater than ΔHv (cf. Table IV). Furthermore, when Rv_0 equals Yv_0 in these two equations, ΔRv equals ΔYv, which equals 1.5 ΔHv (cf. Table IV, exp 1). When Rv_0 is greater than Yv_0 in Eqs. 1 and 2, ΔRv will always be greater than ΔYv (cf. Table IV, exps 2 and 3). Moreover, these equations predict values for ΔRv and ΔYv in exps 2 and 3 in Table IV (from Rv_0, Yv_0, and ΔHv) that differ from the observed values by an average of 8%. Finally, derivation of an expression for ΔHv/(ΔRv + ΔYv) from Eqs. 1 and 2 gives:

$$\Delta Hv/(\Delta Rv + \Delta Yv) = ([Rv_0/2Yv_0] + [Yv_0/2Rv_0] + 2)^{-1}. \quad (3)$$

It can be seen that when Rv_0 is equal to Yv_0, eq. 3 assumes a value of 0.33 (cf. Table IV, exp 1). It can also be seen that this function is relatively insensitive to moderate changes in the Rv_0/Yv_0 ratio. For example, when Rv_0 equals 2 Yv_0, the function assumes a value of 0.31 (cf. Table IV, exps 2 and 3).

While these results clearly indicate that fusion occurs randomly with respect to vacuole type, it remains to be established whether all of the vacuoles actually have equal probabilities of fusing, or whether there are discrete subpopulations within the Rv and Yv classes that are competent for fusion.

It should be emphasized that the factors which control the absolute rate of fusion in a given experiment also remain to be established. While inspection of the data in Table IV shows a correlation between the increases in the magnitudes of ΔRv, ΔYv, and ΔHv with higher total initial vacuole concentrations ($Rv_0 + Yv_0 + Hv_0$), we have also observed that aliquots taken at different times from a given reaction mixture (at 0°C) may exhibit significantly different rates of fusion when incubated at 30–32°C (P. Oates and O. Touster, unpublished observations). This observation indicates that the absolute rate of fusion depends on at least one other factor besides vacuole concentration per se.

The present observations concerning the extent of the increase in vacuole size during the in vitro incubation (see Results) are reinforced by the detection, in a few experiments, of exceedingly large hybrid vacuoles (>75 particles/vacuole) (P. Oates and O. Touster, unpublished observations). Such results indicate that once fusion has occurred between two vacuoles, the vacuole membrane remains capable of participating in further fusion events.

In apparent contrast to our previously reported observation (11), the vacuole membranes were observed in the present study to be stable throughout the course of the in vitro incubation (e.g., Fig. 5 a). This difference appears to be a result of the present use of a more physiological reagent to terminate the reaction (DF), rather than the previously employed 0.15-M salt solution (11). In view of the increasing destabilization of the vacuole membranes by relatively short exposures to KCl concentrations above 30 mM (Fig. 10 a), the previous results do not seem very surprising. However, while the present results clearly indicate that the phenomenon of vacuole rupture does not actually occur in the in vitro reaction mixtures, the previously observed time and temperature dependence of vacuole rupture in the 0.15-M salt-diluted reaction mixtures nevertheless indicates that the sensitivity of the vacuoles to (unphysiological) stress becomes altered during the in vitro incubation.

The present results also demonstrate that the

fusion reaction does not stop after 10 min because of the onset of vacuole rupture per se (11). However, it cannot be ruled out that the factor(s) responsible for decreased vacuole stability under conditions of stress could also be the factor(s) responsible for the cessation of fusion. The reason why the reaction stops after 10 min, although it is currently under investigation, is presently still unknown.

Concerning the effects of KCl (Fig. 10), it should be emphasized that the KCl is added in addition to the endogenous KCl present in the homogenates. While further studies are needed to investigate the specific effects of K^+ and Cl^- on this system, the simplest interpretation of the curve in Fig. 10b rests on the general concept that particular intracellular concentrations of monovalent ions are required for the optimal performance of cellular functions (e.g., reference 6). From the data of Klein (6), it can be estimated that the cytoplasmic concentration of free K^+ in *Acanthamoeba* is ~20 mM. Klein has also reported that when *Acanthamoeba* are suspended in a cold hypotonic medium, the cells lose ~50% of their total K^+ in ~10 min (5). Thus, as a result of the use of cold hypotonic conditions to swell the cells in the present study (see Materials and Methods), a similar depletion in the K^+ content of these homogenates is expected. (This has been confirmed by preliminary atomic absorption measurements [P. Oates and O. Touster, unpublished observations].) In light of these findings, the simplest interpretation of the data in Fig. 10b is that the addition of KCl in amounts >10 mM pushes the total K^+ concentration (and presumably also the Cl^- concentration) over the upper limits of their normal physiological ranges, the increasingly unphysiological conditions causing increasingly stronger inhibition of the fusion reaction, by an as yet unknown mechanism.

Concerning the effects of the metabolic inhibitors which were tested, the lack of effect of KCN and 2,4-DNP suggests that the fusion reaction can proceed in the absence of oxidative metabolism. The basis for the sensitivity of the reaction to F^- (Fig. 11) is presently unknown. While the effect could be because of a suppression of glycolytic metabolism, fluoride is well known to have a number of other biochemical effects, e.g., stimulation of adenyl cyclase (16). Alternatively, a physical chemical effect of F^- on membrane constituents and/or their environment cannot be overlooked.

In conclusion, it is evident that many fundamental questions concerning the biochemistry and biophysics of vacuole fusion in this system await answer. The methods described in this report are presently being applied to some of these questions.

APPENDIX

Derivation of Eqs. 1 and 2

The in vitro fusion reaction proceeds at a constant rate for 10–15 min, after which it ceases (e.g., Fig. 5). It is desired to derive expressions describing the relative changes in Rv, Yv, and Hv which are predicated on random fusion of Rv, Yv, and Hv vacuoles during the time in which fusion is occurring ($t \leq 10$ min). The derivation may be considerably simplified by recognizing that (*a*) since the absolute reaction rates for Rv, Yv, and Hv are constant during this time (above), then the reaction rates relative to one another (the relative reaction rates) are also constant during this time, and (*b*) since the relative reaction rates are constant, then rate equations which describe the initial relative rates will also describe the relative rates throughout the time under consideration ($t \leq 10$ min).

It is assumed that the starting mixture of vacuoles consists predominantly of GGRBC-containing (Rv) and yeast-containing (Yv) vacuoles which are equal in size, shape, and kinetic motion. The initial relative concentration frequencies, r and y, of each vacuole species are defined by $r = Rv_0/Tv_0$ and $y = Yv_0/Tv_0$, where Rv_0 and Yv_0 are the initial concentrations of Rv and Yv respectively, and Tv_0 is the initial total vacuole concentration. If it is assumed that contact between any two vacuoles occurs randomly with respect to vacuole type, then the relative frequencies of Rv-Rv, Rv-Yv, and Yv-Yv contacts which will initially occur among the Rv and Yv vacuoles are given by

$$r^2 + 2ry + y^2, \qquad (1\,a)$$

where r^2 is the relative frequency of Rv-Rv contacts, 2ry is the relative frequency of Rv-Yv contacts, and y^2 is the relative frequency of Yv-Yv contacts. If it is assumed that the relative rate of fusion between the vacuole species is directly proportional to their relative contact frequencies, and that the proportionality constant, k, is independent of the types of interacting vacuoles, then

the initial relative rates of Rv-Rv (RR) fusion ($[dRR/dt]_{i, rel}$), Rv-Yv (RY) fusion ($[dRY/dt]_{i, rel}$), and Yv-Yv (YY) fusion ($[dYY/dt]_{i, rel}$) are given by:

$$(d\ RR/dt)_{i, rel} = k\ r^2 \quad (2a)$$

$$(d\ RY/dt)_{i, rel} = k\ 2ry \quad (2b)$$

$$(d\ YY/dt)_{i, rel} = k\ y^2. \quad (2c)$$

The initial relative rate of loss from the Rv population is given by:

$$(dRv/dt)_{i, rel} = (d\ RR/dt)_{i, rel} + (dRY/dt)_{i, rel} \quad (3a)$$

or, from Eqs. 2 a and 2 b

$$(dRv/dt)_{i, rel} = k(r^2 + 2ry). \quad (4a)$$

Similarly, for the Yv population,

$$(dYv/dt)_{i, rel} = k(y^2 + 2ry). \quad (4b)$$

Likewise, the initial relative rate of increase for the hybrid population is given by:

$$(dHv/dt)_{i, rel} = (d\ RY/dt)_{i, rel} = k\ 2ry. \quad (4c)$$

Since the absolute rate of each process $(dRv/dt)_{abs}$, $(dYv/dt)_{abs}$, and $(dHv/dt)_{abs}$ is constant over $\Delta t \leq 10$ min ($t_0 = 0$), then the rates relative to one another are also constant over $\Delta t \leq 10$ min. Therefore, Eqs. 4 a, 4 b, and 4 c can be written as:

$$(\Delta Rv/\Delta t)_{rel} = k(r^2 + 2ry) \quad (5a)$$

$$(\Delta Yv/\Delta t)_{rel} = k\ (y^2 + 2ry) \quad (5b)$$

$$(\Delta Hv/\Delta t)_{rel} = k2ry. \quad (5c)$$

Dividing Eqs. 5 a and 5 b by 5 c and multiplying each by ΔHv gives:

$$\Delta Rv = ([r/2y] + 1)\Delta Hv \quad (6a)$$

$$\Delta Yv = ([y/2r] + 1)\Delta Hv \quad (6b)$$

or, recalling the definitions of r and y,

$$\Delta Rv = ([Rv_0/2Yv_0] + 1)\Delta Hv \quad (7a)$$

and,

$$\Delta Yv = ([Yv_0/2Rv_0] + 1)\Delta Hv, \quad (7b)$$

which are Eqs. 1 and 2, respectively.

The authors are very grateful to Dr. Robert J. Neff, who generously provided us with the use of his cell culture facilities throughout the course of this work. We also wish to acknowledge the very capable technical assistance of Ms. Charlotte Foster.

This work was supported in part by grant 2-RO1-CA-07489 from the National Cancer Institute, United States Public Health Service, to O. Touster, and in part by a Dr. Chaim Weizmann Postdoctoral Fellowship for Scientific Research to P. J. Oates.

Received for publication 6 October 1977, and in revised form 31 March 1978.

REFERENCES

1. Baudhuin, P., P. Evrard, and J. Berthet. 1967. Electron microscopic examination of subcellular fractions. I. The preparation of representative samples from suspensions of particles. *J. Cell Biol.* **32**:181–191.
2. Cotman, C. W., and D. A. Flansburg. 1970. An analytical micromethod for electron microscopic study of the composition and sedimentation properties of subcellular fractions. *Brain Res.* **22**:152–156.
3. De Duve, C. 1969. The lysosome in retrospect. *In* Lysosomes in Biology and Pathology. J. T. Dingle and H. B. Fell, editors. North-Holland Publishing Co., Amsterdam. **1**:3–40.
4. De Duve, C., and R. Wattiaux. 1966. Functions of lysosomes. *Annu. Rev. Physiol.* **28**:435–492.
5. Klein, R. L. 1959. Transmembrane flux of K^{42} in *Acanthamoeba* sp. *J. Cell Comp. Physiol.* **53**:241–258.
6. Klein, R. L. 1961. Homeostatic mechanisms for cation regulation in *Acanthamoeba* sp. *Exp. Cell Res.* **25**:571–584.
7. Lucy, J. A. 1973. The chemically-induced fusion of cells. *In* Membrane Mediated Information. P. W. Kent, editor. American Elsevier Publishing Co., Inc., New York. **2**:117–128.
8. Luft, J. H. 1961. Improvements in epoxy resin embedding methods. *J. Biophys. Biochem. Cytol.* **9**:409–414.
9. Maunsbach, A. B. 1966. Isolation and purification of acid phosphatase-containing autofluorescent granules from homogenates of rat kidney cortex. *J. Ultrastruct. Res.* **16**:13–34.
10. Oates, P. J., and O. Touster. 1976. A new method for preparing subcellular materials for quantitative measurements by electron microscopy. *J. Cell Biol.* **70**(2, Pt. 2):206 a. (Abstr.).
11. Oates, P. J., and O. Touster. 1976. In vitro fusion of *Acanthamoeba* phagolysosomes. I. Demonstration and quantitation of vacuole fusion in *Acanthamoeba* homogenates. *J. Cell Biol.* **68**:319–338.
12. Poste, G., and A. C. Allison. 1973. Membrane fusion. *Biochem. Biophys. Acta.* **300**:421–465.
13. Robbie, W. A. 1946. The quantitative control of cyanide in manometric experimentation. *J. Cell Comp. Physiol.* **27**:181–209.
14. Schober, R., C. Nitsch, U. Rinne, and S. J. Morris. 1977. Calcium-induced displacement of membrane-associated particles upon aggregation of chromaffin granules. *Science (Wash. D. C.)* **195**:495–497.
15. Sjöstrand, F. S. 1967. Electron Microscopy of Cells and Tissues. Academic Press Inc., New York. **1**:436–447.
16. Sutherland, E. W., T. W. Rall, and T. Menon. 1962. Adenyl cyclase. I. Distribution, preparation, and properties. *J. Biol. Chem.* **237**:1220–1227.
17. Wetzel, M. G., and E. D. Korn. 1969. Phagocytosis of latex beads by *Acanthamoeba castellanii* (Neff). III. Isolation of the phagocytic vesicles and their membranes. *J. Cell Biol.* **43**:90–104.
18. Worsfold, M., R. F. Dunn, and J. B. Peter. 1969. A simplified technique for preparing isolated subcellular particles for electron microscopy. *J. Lab. Clin. Med.* **74**:160–165.